International Journal of Engineering and Technical Research (IJETR)
ISSN: 2321-0869, Volume-3, Issue-5, May 2015

Effect of Changing Frequency and Power Factor on Performance of Solar PV Grid Tied Systems

Satvinder Singh, Neha Sharma, Akhil Gupta

Abstract— **In this paper, the model of the Photovoltaic (PV) array has been explained in which the basic current and voltage equations for a PV cell have been defined. It is discussed that output response of PV system depends upon incident solar radiation and ambient temperature. The modeling of solar PV single stage grid connected system at different power factors is done. The nature of real power generated by solar PV array through converter has been shown and proved that, whenever the power from grid is un available, the real power requirement of the load is achieved by converter. Maximum Power point Tracking (MPPT) technique in which data through look up table is used through which behavior of actual DC link voltage is discussed. Finally, the simulation of proposed system is performed under two different cases. In first case, the effect of changing power factor on active power, reactive power and Total Harmonic Distortion (THD) values is observed. It is found that the THD of grid current increases with increase in the phase angle of grid current converter voltage. It affects the active power flow among converter, load and utility grid. In the second case, the effect of changing frequency on active power, reactive power and THD values is noticed. It is observed that the THD of converter current increases, whereas, the THD of grid current remains constant.**

Index Terms— **Photovoltaic, harmonic, power factor, power and frequency**

I. INTRODUCTION

The non-renewable energy sources and fossil fuels such as coal, petroleum and natural gas have been extensively employed for thousands of years on the earth. After their burning, these fossil fuel produces excessive heat which results severe environmental pollutions such as air pollution, water pollution, and soil pollution. The fast depletion of the fossil fuels may lead to shortage of ever increasing electrical power demand of the world for various domestic and industrial applications. This leads electric power engineers and researchers to think for alternative available renewable resources such as wind, Photovoltaic (PV), Fuel Cells (FC), etc.

The conventional Maximum Power Point Tracking (MPPT) methods can be classified into number of categories as mentioned in [1]. From the literature survey, the first category consists of constant voltage or current reference methods. In this, the controller sets the voltage or current reference to an empirical ratio of the open circuit voltage or short circuit current. Although it is very simple and quick method, but can't extract maximum power under all environmental conditions and has a low tracking efficiency [2]. The second category consists of the Perturbation and Observation (P&O) method. P&O MPPT method use the idea of hill climbing algorithm. It works well, when the solar radiation does not vary rapidly with time. Due to simplicity and ease of implementation, it is most widely applied methods in PV industry. However, their drawbacks are slow tracking speed and oscillations around Maximum Power Point (MPP) [3]. To reduce or eliminate these drawbacks, P&O methods have been improved by using variable step-sizes [4].

Another disadvantage with P&O MPPT method is that when the environmental conditions change rapidly, i.e. when the solar radiation changes rapidly, the operating point may deviate from the MPP by tracking towards a wrong direction. This is because the algorithms are not able to distinguish between changes caused by the perturbation or by the changing environmental conditions. Various methods to overcome this problem have been proposed in references [5-6]. The third MPPT category is the Incremental Conductance (IC) method [3]. This method tracks faster and has a better performance than the P&O method, especially under rapidly changing atmospheric conditions. There are also some other MPPT algorithms. For example, an MPPT method which senses the output voltage or current of converter is presented in [7]. The Pulse Width Modulation (PWM) based converter is modeled as a time-varied transformer, so that the input voltage or current can be calculated from the output voltage or current. By analyzing linear and non-linear loads, it was found that for loads with non-negative incremental impedance, the output current and voltage increases monotonically as the output power increases. Thus maximum output current (or voltage) implies maximum output power. Therefore, the MPPT algorithm can be implemented based only on a single output parameter, which can simplify hardware design and control algorithm. With this method, it is the output power of Voltage Source Converter (VSC) that is maximized, rather than the solar PV array power. Thus solar PV array may be operating slightly off the MPP, but the total efficiency is optimized. The characteristics of solar radiation are found to be constantly variable. The atmospheric conditions, climate, and geographic characteristics are most important parameters, which determine the solar radiation quantity received on a given point of the earth [8-10].

II. BASIC MODELING OF SOLAR PV SYSTEM

As mentioned in reference [11], for a known temperature and a known solar radiation level, a model is obtained which is then modified to handle different cases of temperature and solar radiation levels. The solar cell

Satvinder Singh, Electrical Engineering M.Tech. scholar at EE Department, GGS College of Modern Technology, Kharar, Mohali, India

Neha Sharma, Electrical Engineering Assistant Professor, EE Department,, GGS College of Modern Technology, Kharar, Mohali, India

Akhil Gupta, Associate Professor, Electrical Engineering Department, Chandigarh University, Kharar, Mohali, India

operating temperature varies as a function of solar radiation level, and ambient temperature. The variable ambient temperature affects the cell output voltage, and cell photocurrent. These effects are represented in the model by Equations (1)-(2) as:

$$C_{tv} = 1 + \beta_t (T_a - T_x) \quad \textbf{(1)}$$

$$C_{ti} = 1 + \gamma \frac{(T_x - T_a)}{S_c} \quad \textbf{(2)}$$

where, β_t = 0.0042 and γ = 0.062 for the cell used, and T_a = 200 ˚C, is ambient temperature during the cell testing. This is used to obtain the modified model of cell for another ambient temperature T_x. A change in solar radiation causes a change in cell photocurrent, and operating temperature, which in turn affects cell output voltage. If solar radiation increases from S_{x1} to S_{x2}, cell operating temperature and photocurrent will also increase from T_{x1} to T_{x2} and from I_{phl} to I_{ph2}, respectively. Thus change in operating temperature and photocurrent due to variation in solar radiation are expressed as,

$$C_{sv} = 1 + \beta_t \alpha_s (S_x - S_c) \quad \textbf{(3)}$$

$$C_{si} = 1 + \frac{(S_x - S_c)}{S_c} \quad \textbf{(4)}$$

where, S_c is benchmark reference solar radiation level during cell testing to obtain modified cell model. S_x is new level of solar radiation. The constant α_s represents slope of change in cell operating temperature due to change in solar radiation level and is equal to 0.011 for solar cells used. Using Equations (1)-(4), the new values of cell output voltage V_{an} and photocurrent I_{phn} at new temperature T_x and solar radiation S_x are obtained as,

$$V_{an} = C_{tv} C_{sv} V_a \quad \textbf{(5)}$$

$$I_{phn} = C_{ti} C_{si} I_{ph} \quad \textbf{(6)}$$

V_a and I_{ph} are benchmark reference cell output voltage and reference cell photocurrent, respectively.

The *I-V* and *P-V* curves for changing solar radiation but a fixed temperature (25 ˚C) is shown in Figure 1 (a) and Figure 1(b), respectively. The *I-V* curve it is found that there are two regions in the curve: one is current source region whereas other is voltage source region. In the voltage source region (in right side of the curve), the internal impedance is low whereas, in current source region (in the left side of the curve), the impedance is high. Solar radiation and ambient temperature plays an important role in predicting the *I-V* characteristic. The effects of both factors are considered during the designing of PV system. Whereas the solar radiation affects the output, temperature mainly affects the terminal voltage. Figure 2 (a) and Figure 2 (b) gives the simulated *I-V* and *P-V* characteristic for various temperatures at a fixed irradiance at 1000 W/m^2, respectively.

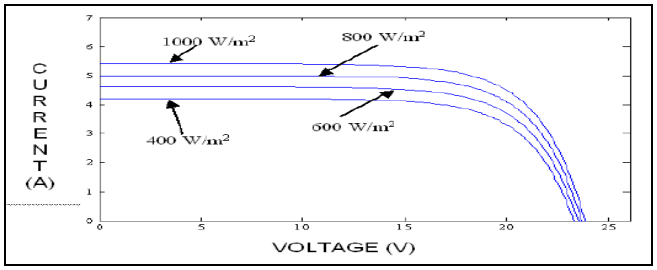

(a)

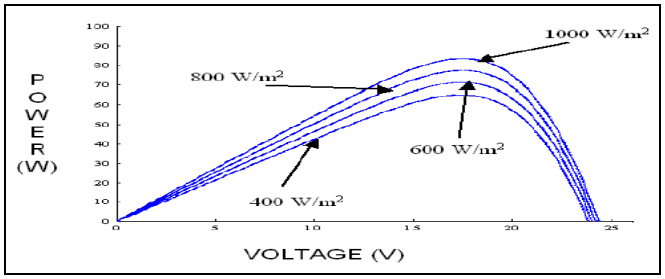

(b)

Figure 1 (a) *I-V* and (b) *P-V* characteristic, of a solar array for a fixed temperature but varying irradiance

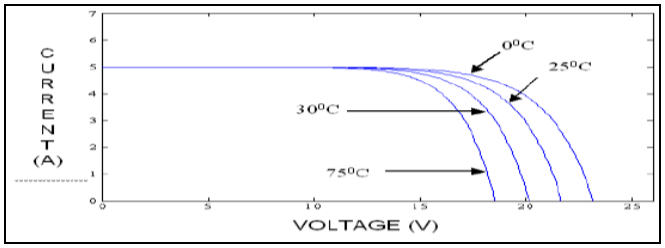

(a)

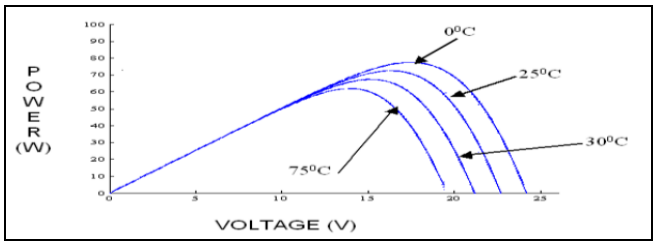

(b)

Figure 2 (a) *I-V* and (b) *P-V* characteristic of a PV array under a fixed irradiance but varying temperatures

A. CONFIGURATION OF SOLAR PV SYSTEM

As shown in Figure 3, the Power Conditioning System (PCS) is comprised of VSC along with its control, MPPT control; Phase Locked Loop (PLL) and *LCL* filter for the removal of harmonics. PLL algorithm is used for grid synchronization. The output of the VSC is connected to grid through a inductance so that the flow of power can take place on both sides. The presence of inductance creates a phase angle which is responsible for the flow of active and reactive from both sides. A look-up table is used in Matlab simulation in which the data is fed for the voltage at MPP. The data which has been used is 600, 700, 800, 900, 1000,1100 and 1200 V at various solar radiation range 88, 90, 92, 94, 96, 98

and 100 W/m^2. No. of series and parallel connected PV cells are 2200 and 26, respectively. The three phase series RLC load used is 440 V,50 Hz, P=63 kW, Q=20 kW (+ve). DC voltage regulator gains are 0.45 and 18, whereas DC current regulator gains are 0.026 and 5.

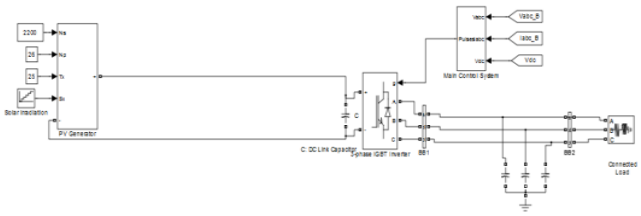

Figure 3 Simulated solar PV system connected with load

III. SIMULATION RESULTS AND DISCUSSION

For the proposed system, the total simulation time period is 0.3 s. Figure 4 (a) shows the nature of the solar radiation which acts as input to the proposed system. Since array current is directly proportional to the solar radiation, its nature is approximately proportional to the solar radiation curve, Figure 4 (b). Figure 4 (c) gives the PV array voltage, whereas Figure 4 (d) shows the PV array power. The output power of PV array is product of PV array voltage and current. It is possible to observe that the approximate value of the PV array power is 48 kW.

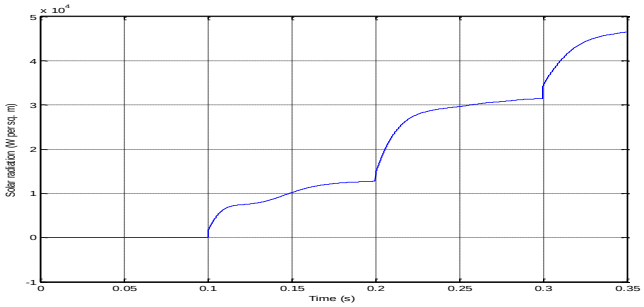

(a)

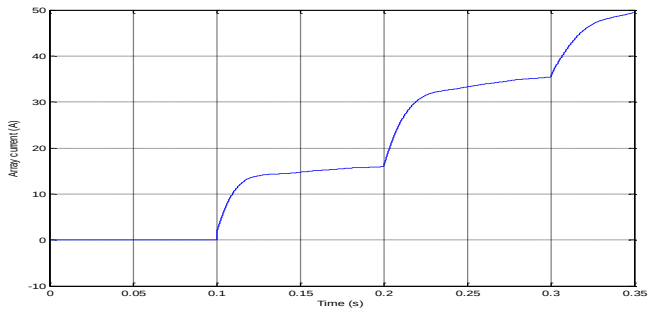

(b)

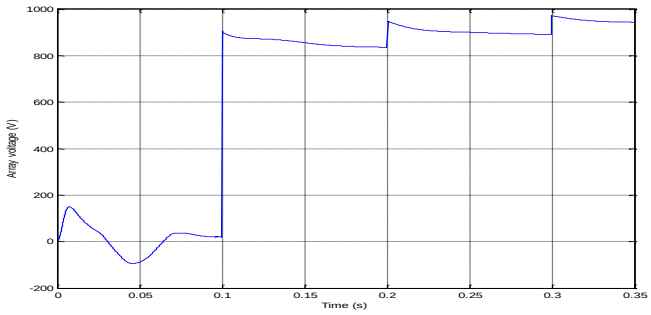

(c)

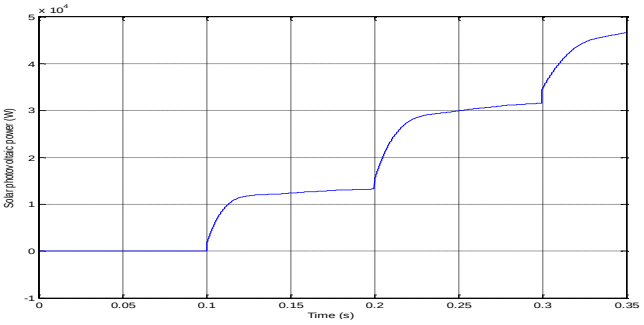

(d)

Figure 4 (a) Solar radiation (b) Solar array current (c) Solar array voltage (d) Solar array power

Figure 5 (a) depicts the nature of actual DC link voltage around the reference MPPT voltage. The blue line indicates the tracking of actual DC link voltage around reference voltage. As the ambient temperature T_x increases and solar radiation increases, the actual value closely follows the reference voltage. The initial transients can be controlled by the further tuning of PI controllers. Figure 5 (b) shows that as the solar radiation level increases the grid power decreases. The power requirement of the load is met by PV array through VSC converter. This has been shown by Figure 5 (c), which depicts the VSC power. Figure 5 (d) shows the variation of the modulation index.

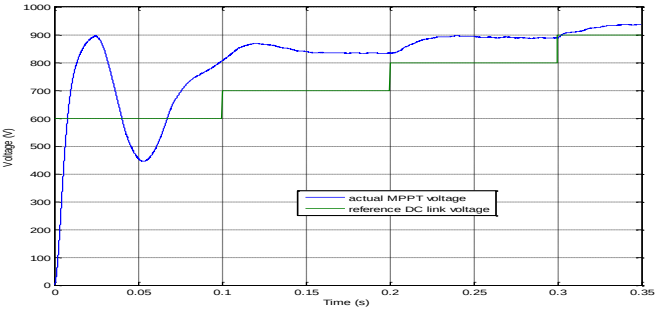

(a)

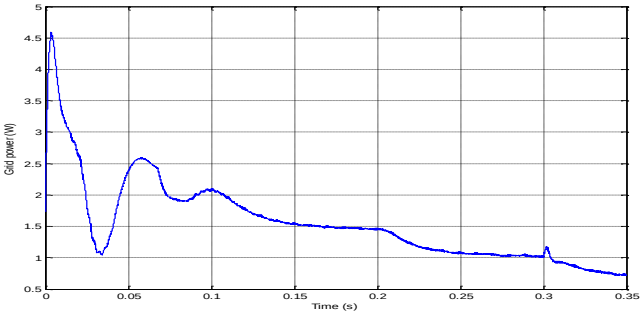

(b)

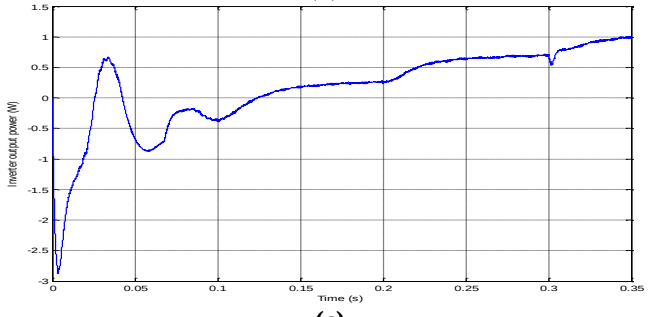

(c)

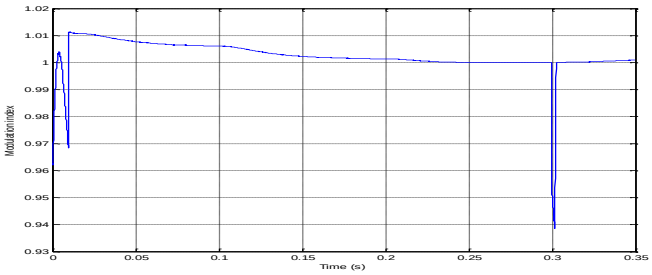

(d)

Figure 5 (a) Actual DC link voltage and MPPT reference voltage (b) Grid output power (c) Inverter output power (d Modulation index

The performance of the system is evaluated at different power factors and frequencies. The total simulation period has been chosen as t = 0.35 s. The following are the two case studies:

Case I at different power factors and same frequency; Case II at different frequencies and same power factors.

A. Case I at different power factors and same frequency

- ***at unity power factor, 440 V, 50 Hz***

As shown in Figure 6 (a), the active power is generated at different temperature and solar radiation, at unity power factor. The system has been tested at constant frequency of 50 Hz. This active power has been generated according to data generated through MPPT used through look-up table. The grid power completes the load power demand. As it decreases, the load power demand is met with the solar PV array through the IGBT based converter system. The initial transient at t = 0.02 s can be more controlled by introducing tuning of PI controllers. Similarly, the reactive power response has been shown in Figure 6 (b). Reactive power compensation of the load is done by solar PV through converter system (shown by blue line). At t = 0.05 s, the reactive power generated by grid decreases till t = 0.35 s. The reactive power of the load is shown as constant at 20 kVAR.

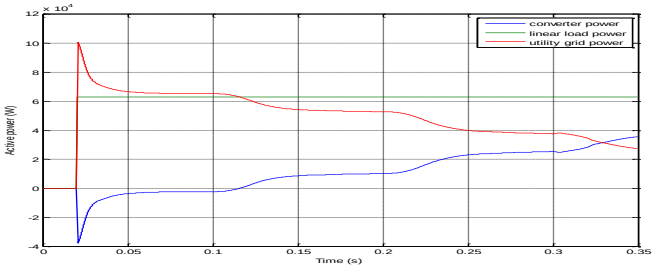

(a)

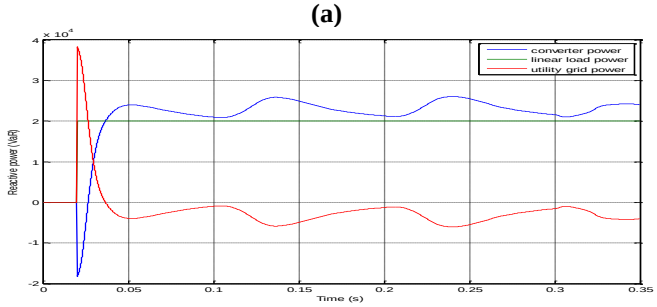

(b)

Figure 6 (a) Active power (b) Reactive power, variation of VSC, load and utility grid (Unity power factor, 50 Hz)

THD values from Fast Fourier Transform (FFT) analysis for VSC current and grid injected current are found to be 1.05 % and 0.49 %, respectively.

- *at power factor = 0.866, 440 V, 50 Hz*

As depicted by Figure 7 (a), there has been a non-uniformity in the active power generation between the period t = 0.07 s to t = 0.1 s, which is due to decrease in the power factor from unity to 0.866. This is due to the fact, that the power factor is directly proportional to active power. Similar behavior has been shown by reactive power response between the period t = 0.02 s to t = 0.1 s, Figure 7 (b).

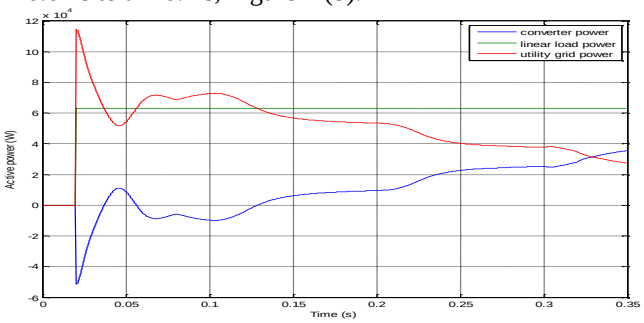

(a)

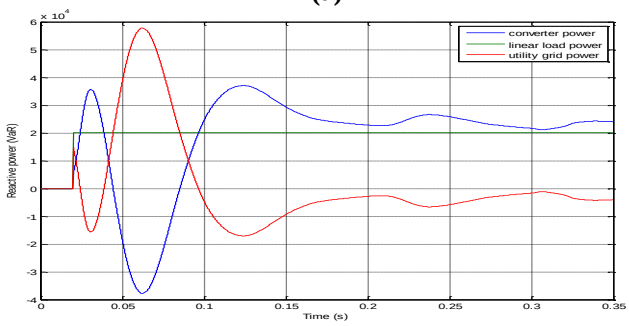

(b)

Figure 7 (a) Active power (b) Reactive power, variation of VSC, load and utility grid (Power factor=0.866, 50 Hz)

The THD response of VSC current and grid injected current at 0.866 power factor, respectively. The THD values are found to be 7.19 % and 2.71 %, respectively. Thus there has been the increase in THD with decrease in power factor.

- *at power factor = 0.707, 440 V, 50 Hz*

At 0.707 power factor, the response becomes more oscillatory as shown by active power generated by solar PV through converter system, Figure 8 (a). The maximum power generated by utility grid is 80 KW. However, there has been decrease in the overshoots in the reactive power response after t = 0.15 s, Figure 8 (b).

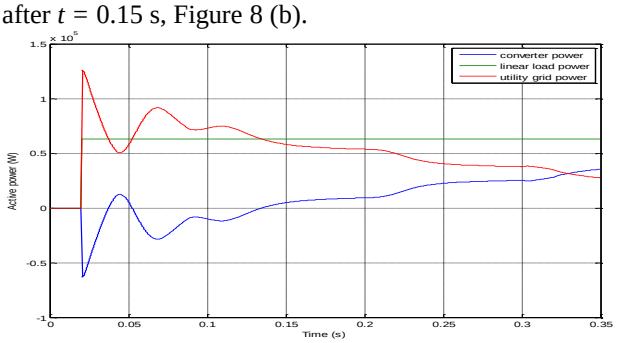

(a)

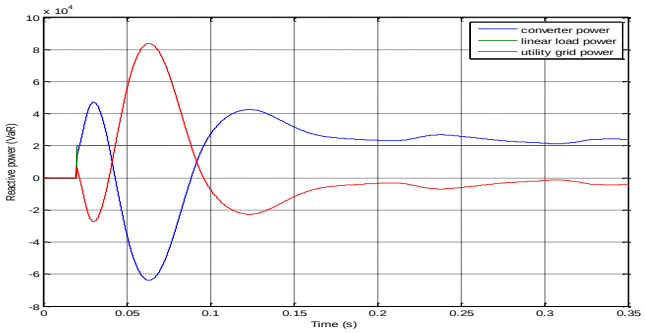

(b)

Figure 8 (a) Active power (b) Reactive power, variation of VSC, load and utility grid (Power factor=0.707, 50 Hz)

The THD values are found to be 8.28 % and 2.67 %, respectively. Again, there has been the increase in the THD of VSC current with decrease in power factor.

- *at power factor = 0.5, 440 V, 50 Hz*

Figure 9 (a) depicts that the overshoot increases to 1.2×10^5. Thus the oscillatory response increases with the decrease in operating power factor. From Figure 9 (b), the reactive power generated by utility grid is 1.1×10^5. However, in this case, the compensation is met with the grid power from 0.04 s to 0.08 s, thereafter, completed by reactive power generated by VSC.

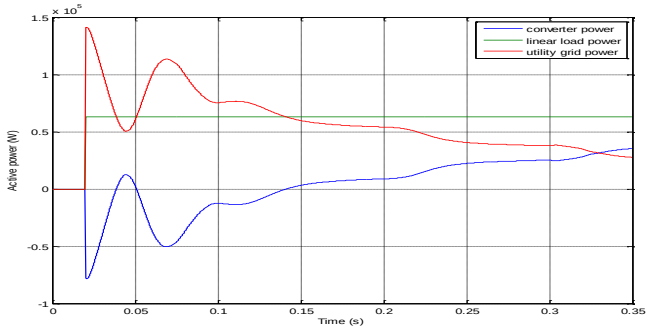

(a)

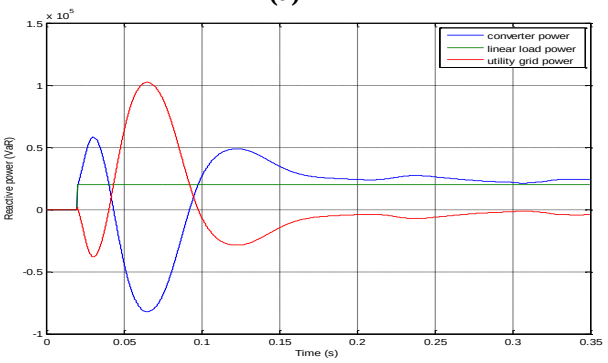

(b)

Figure 9 (a) Active power (b) Reactive power, variation of VSC, load and utility grid (Power factor=0.50, 50 Hz)

The THD values are found to be 9.68% and 2.58%, respectively. Thus, it has been found that there has been the increase in the THD of VSC current from 1.05% to 9.68% as the power factor decreases.

B. Case II at different frequency and same power factors

This sub-section presents the behavior of proposed system at unity power factor and two different frequencies.

- *at unity power factor, 440 V, 49 Hz*

Figure 10 (a) depicts the active power response whereas; Figure 10 (b) depicts the reactive power response of VSC, load and utility grid. The THD values of VSC current and grid current are found to be 0.49% and 1.84%, respectively.

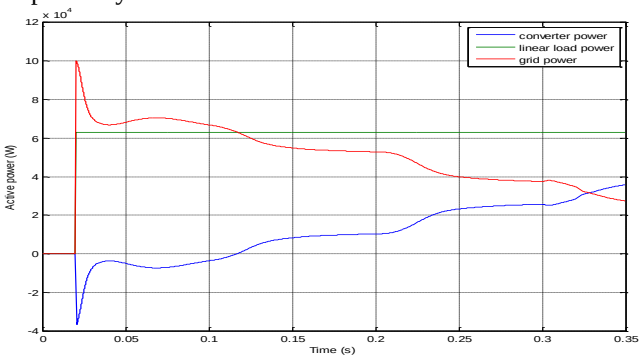

(a)

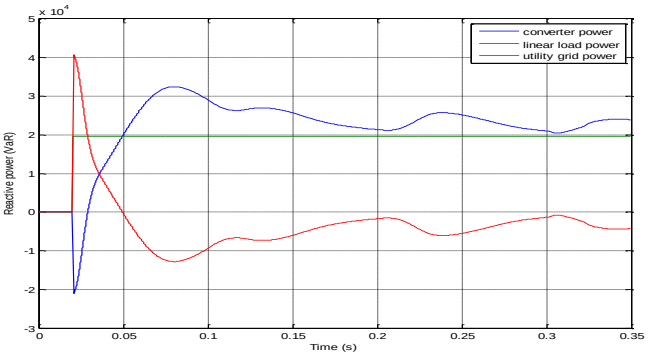

(b)

Figure 10 (a) Active power (b) Reactive power, variation of VSC, load and utility grid (Unity power factor, 49 Hz)

- *at unity power factor, 440 V, 51 Hz*

Figure 11 (a) depicts the active power response whereas; Figure 11 (b) depicts the reactive power response of VSC, load and utility grid. The THD values of VSC current and grid current are found to be 6.52% and 1.84%, respectively. This it has is concluded that change in frequency has no effect on the THD of grid current whereas, THD of VSC current has been increased from 0.49% to 6.52%.

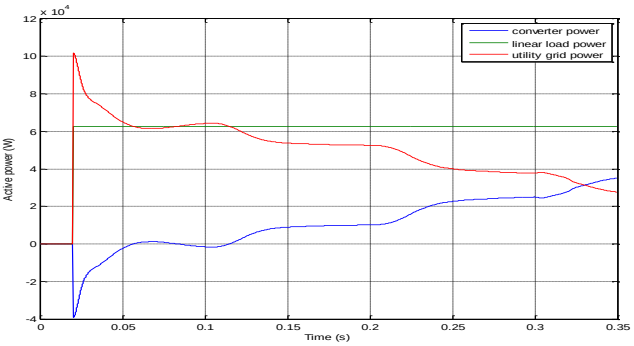

(a)

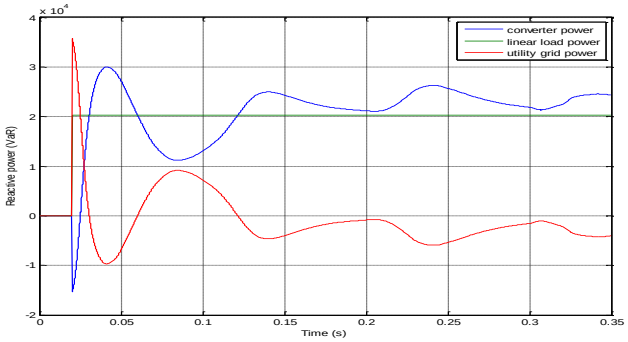

(b)

Figure 11 (a) Active power (b) Reactive power, variation of VSC, load and utility grid (Unity power factor, 51 Hz)

IV. CONCLUSION

In this paper, the simulation of the proposed system is performed under two different cases. In first case, the effect of changing power factor on active power, reactive power and THD values is observed. It is observed that the THD of grid current increases with increase in the phase angle of grid current VSC voltage. It affects the active power flow among VSC, load and utility grid. In the second case, the effect of changing frequency on active power, reactive power and THD values is noticed. It is observed that the THD of VSC current increases whereas, the THD of grid current remains constant.

REFERENCES

[1] T. Esram, and P.L. Chapman, "Comparison of photovoltaic array maximum power point tracking techniques", *IEEE Trans. on Energy Conversion*, vol. 22, no. 2, pp. 439-449, June 2007.

[2] D. P. Hohm and M. E. Ropp, "Comparative study of maximum power point tracking algorithms", *Progress in Photovoltaics: Research and Application*, vol. 11, pp. 47- 62, 2003.

[3] K. H. Hussein, I. Muta, T. Hoshino, and M. Osakada, "Maximum photovoltaic power tracking: an algorithm for rapidly changing atmospheric conditions", *IEE Proceedings, Generation, Transmission and Distribution*, vol. 142, no. 1, pp. 59-64, Jan. 1995.

[4] N. Khaehintung, T. Wiangtong, and P. Sirisuk, "FPGA implementation of MPPT using variable step-size P&O algorithm for PV applications", In: International Symposium on Communications and Information Technologies, ISCIT, pp. 212-215, 2006.

[5] S. Jain, and V. Agarwal, "A new algorithm for rapid tracking of approximate maximum power point in photovoltaic systems", *IEEE Power Electronics Letters*, vol. 2, no. 1, pp. 16-19, March 2004.

[6] D. Sera, R. Teodorescu, J. Hantschel, and M. Knoll, "Optimized maximum power point tracker for fast-changing environmental conditions", *IEEE Trans. on Industrial Electronics*, vol. 55, no. 7, pp. 2629-2637, July 2008.

[7] D. Shmilovitz, "On the control of photovoltaic maximum power point tracker via output parameters", *IEE Proceedings on Electric Power Application*, vol. 152, no. 2, pp. 239-248, March 2005.

[8] I. Muhammad. An introduction to solar radiation, Academic Press, New York 1983.

[9] R. Almanza Salgado, V. Estrada-Cajigal Ramirez, and J. Barrientos Avila, "Update of the maps of global irradiation to pave in the mexican republic", Series of the Institute of Engineering no. 547.2007.

[10] A.S. Drigas, J. Vrettaros, L.G. Koukianakis, and J.G. Glentzes, "A Virtual Lab and e-learning system for renewable energy source", In: Proc. of the 1st WSEAS/IASME Int. Conf. on Educational Technologies, Tenerife, Canary Islands, Spain, Dec. 16-18, 2005.

[11] H. Altas, and A.M. Sharaf, "A photovoltaic array simulation model for Matlab-Simulink GUI environment", In: Proc. of IEEE Int. Conf. on Clean Electrical Power, Capri, pp. 341-345, May 21-23, 2007.

Mr. Satvinder Singh received his B.Tech. (EE) from RIEIT, Railmajra. He is Assistant Professor at Electrical Engg department at RIEIT, Railmajra, near Ropar, Punjab. He is the post graduate student at Guru Gobind Singh College of Modern Technology, Mohali, Punjab. He is having around 3 years and 10 months experience in academics. His areas of research are renewable energy systems, power electronics and power systems.

Ms. Neha Sharma is Assistant Professor and Coordinator (EE) at Guru Gobind Singh College of Modern Technology Kharar, Mohali. She is having 1 year 8 months experience and has obtained his M.Tech (Instrumentation and Control) from BBSBEC, Fatehgarh Sahib (PTU, Jalandhar).

Mr. Akhil Gupta received B.E (Electrical Engg) from GZSCET, Bathinda (PTU, Jalandhar) in 1999 and M.Tech in Electrical Engineering from Kay Jay group of Institutes, Patiala (Institute of Advanced Studies In Education, Rajasthan) in 2005. He is now working as Associate Professor in Chandigarh University, Gharuan, District Mohali, Punjab, India. He has above 15 years of experience in academics and industry. His area of research is in the application of renewable energy systems into electrical power systems, and controls